

RESEARCH

Open Access



A modular pathway engineering strategy for the high-level production of β -ionone in *Yarrowia lipolytica*

Yanping Lu, Qingyu Yang, Zhanglin Lin* and Xiaofeng Yang*

Abstract

Background: The GRAS and oleaginous yeast *Yarrowia lipolytica* (*Y. lipolytica*) is an attractive cell factory for the production of chemicals and biofuels. The production of many natural products of commercial interest have been investigated in this cell factory by introducing heterologous biosynthetic pathways and by modifying the endogenous pathways. However, since natural products anabolism involves long pathways and complex regulation, re-channelling carbon into the product of target compounds is still a cumbersome work, and often resulting in low production performance.

Results: In this work, the carotenogenic genes contained *carB* and bi-functional *carRP* from *Mucor circinelloides* and carotenoid cleavage dioxygenase 1 (*CCD1*) from *Petunia hybrida* were introduced to *Y. lipolytica* and led to the low production of β -ionone of 3.5 mg/L. To further improve the β -ionone synthesis, we implemented a modular engineering strategy for the construction and optimization of a biosynthetic pathway for the overproduction of β -ionone in *Y. lipolytica*. The strategy involved the enhancement of the cytosolic acetyl-CoA supply and the increase of MVA pathway flux, yielding a β -ionone titer of 358 mg/L in shake-flask fermentation and approximately 1 g/L (~280-fold higher than the baseline strain) in fed-batch fermentation.

Conclusions: An efficient β -ionone producing GRAS *Y. lipolytica* platform was constructed by combining integrated overexpressed of heterologous and native genes. A modular engineering strategy involved the optimization pathway and fermentation condition was investigated in the engineered strain and the highest β -ionone titer reported to date by a cell factory was achieved. This effective strategy can be adapted to enhance the biosynthesis of other terpenoids in *Y. lipolytica*.

Keywords: Metabolic engineering, β -ionone, PK-PTA pathway, Acetyl-CoA, Fermentation optimization, Dissolved oxygen, *Yarrowia lipolytica*

Background

Terpenoids and their derivatives have attracted great interest for their commercial application as biofuels, flavoring ingredients, fragrances, antiseptics and pharmaceuticals [1–4]. β -ionone, an apocarotenoid derived

from carotenoids (C40 terpenoids), has a warm, woody, and violet-like aroma, a low odor threshold, and has been widely used in the food and cosmetic industries [5]. Moreover, β -ionone is a key intermediate for the synthesis of vitamins A, E and K [6]. Currently, the annual production of β -ionone is about 4000–8000 tonnes and the demand is rapidly increasing [1]. Due to the long grow cycle and low concentration in plants, the direct extraction of β -ionone from plants affords low yields of the terpenoid, insufficient to meet the demand [4, 7].

*Correspondence: zhanglinlin@scut.edu.cn; biyangxf@scut.edu.cn
School of Biology and Biological Engineering, South China University of Technology, 382 East Outer Loop Road, University Park, Guangzhou 510006, China



© The Author(s) 2020. This article is licensed under a Creative Commons Attribution 4.0 International License, which permits use, sharing, adaptation, distribution and reproduction in any medium or format, as long as you give appropriate credit to the original author(s) and the source, provide a link to the Creative Commons licence, and indicate if changes were made. The images or other third party material in this article are included in the article's Creative Commons licence, unless indicated otherwise in a credit line to the material. If material is not included in the article's Creative Commons licence and your intended use is not permitted by statutory regulation or exceeds the permitted use, you will need to obtain permission directly from the copyright holder. To view a copy of this licence, visit <http://creativecommons.org/licenses/by/4.0/>. The Creative Commons Public Domain Dedication waiver (<http://creativecommons.org/publicdomain/zero/1.0/>) applies to the data made available in this article, unless otherwise stated in a credit line to the data.

Commercial β -ionone is mainly produced by chemical synthesis, which is characterized by the formation of undesirable byproducts and is not environmentally friendly [8]. These concerns have stimulated increased efforts to develop microbial cell factories for the production of natural products from carbohydrate feedstocks. The use of generally recognized as safe (GRAS) microorganisms to convert natural raw materials into products leads to aroma compounds that can be described as natural, if these compounds are known to be components of the natural raw materials, according to the United States and the European Union flavor regulations [9]. As a consequence, companies and researchers have shifted their focus from *Escherichia coli* (*E. coli*) to GRAS microorganisms, such as yeasts, for terpenoids production [10–13].

Recently, the GRAS, unconventional yeast *Y. lipolytica* has rapidly emerged as a valuable cell factory for the production of terpenoids due to its own endogenous mevalonate pathway (MVA) and its high lipid production capacity [7, 12]. Metabolic engineering and synthetic biology offer the ability of rewiring microbial carbon fluxes to create efficient cell factories for the production of natural products. To date, this yeast has been successfully engineered for the production of monoterpenoids, e.g. 23.6 mg/L limonene [14] and 7.0 mg/L linalool [15], sesquiterpenoids, e.g. 978.2 μ g/L (+)-nootkatone [16], and tetraterpenoids, e.g. 242.0 mg/L lycopene [17], 6.5 g/L β -carotene [18] and 54.6 mg/L astaxanthin [19].

In microbial cell factories engineered for commercial production, pathway design and optimization are essential steps [20, 21]. Ajikumar et al. [22] established a multivariate modular metabolic engineering (MMME) approach, which segments metabolic pathways into modules regulated by distinct promoters, to enhance taxadiene (a taxol intermediate) production by ~15,000 fold in *E. coli*. Variations of this modularization strategy have been implemented in *E. coli* [23, 24] and in *S. cerevisiae* [25, 26].

Additionally, efficient and predictable synthetic biology tools have been developed that facilitate the metabolic engineering of *Y. lipolytica*. Popular approaches for assembling the different DNA parts into gene cassettes, such as Gibson assembly, Gateway and Golden Gate strategies, have also been applied to the engineering of *Y. lipolytica* [18, 27]. These gene cassettes can be further simplified and efficiently edited by the powerful tool CRISPR–Cas9, which was implemented at 2016 [28]. The CRISPR interference (CRISPRi) system was also established for gene expression modification in *Y. lipolytica* [29].

In this study, we used a modular pathway engineering approach for the construction and optimization of a long metabolic pathway, for the overproduction of β -ionone in *Y. lipolytica*. The whole pathway was divided into three modules, which were then segmented into a total of seven units for genome integration (Fig. 1). These units

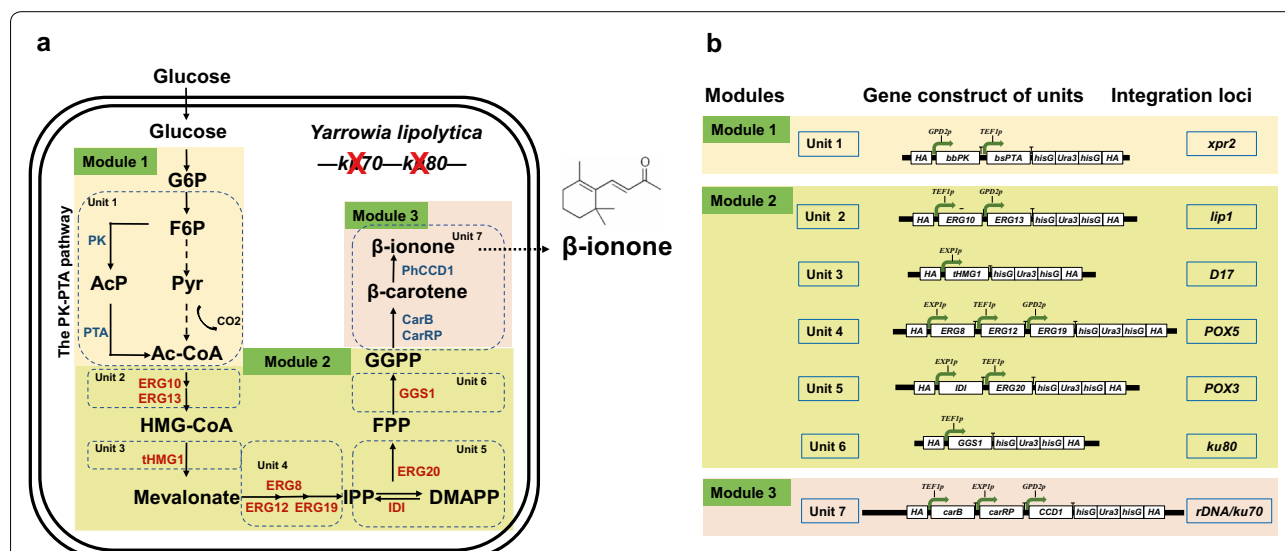


Fig. 1 β -ionone biosynthesis pathway in the engineered *Yarrowia lipolytica*. **a** The biosynthesis pathway was organized into three modules: Module 1, the cytosolic acetyl-CoA supply module; Module 2, the MVA module; Module 3, the β -ionone synthesis module. Exogenous and endogenous genes are indicated in blue and red, respectively. **b** The detailed view of all the seven units. The genes expressed encode the following enzymes: *PK* phosphoketolase, *PTA* phosphotransacetylase, *ERG10* acetoacetyl-CoA thiolase, *ERG13* hydroxymethylglutaryl-CoA synthase, *thMG1* truncated hydroxymethylglutaryl-CoA reductase, *ERG8* phosphomevalonate kinase, *ERG12* mevalonate kinase, *ERG19* mevalonate diphosphate decarboxylase, *IDI* isopentenyl diphosphate isomerase, *ERG20* geranyl/farnesyl diphosphate synthase, *GGI1* GGPP synthase, *carB* phytoene dehydrogenase, *carRP* phytoene synthase/lycopene cyclase, *CCD1* carotenoid cleavage dioxygenase

and modules were designed to enable quick assembly, integration and step-wise evaluation of the β -ionone synthesis pathway in *Y. lipolytica*. The best performing strain yielded 358 mg/L β -ionone accumulation in shake-flask fermentation and 0.98 g/L in fed-batch fermentation using a 3-L bioreactor, the highest titers for β -ionone obtained in microbial cell factories reported to date. During the course of this work, Czajka et al. [30] engineered *Y. lipolytica* to produce 68 mg/L in flask fermentation and 380 mg/L in a 2-L bioreactor by the integrated over-expression of the MVA and β -ionone synthesis pathway genes, and fermentation optimization. In this work, we applied a different modular integration approach that allowed for evaluation of different units of the genes along the whole pathway, and used the CRISPR–Cas9 technique, which is more convenient than the Cre-loxP technique [30]. In particular, we introduced a new factor, the acetyl-CoA supply module, to increase the availability of acetyl-CoA in the cytosol. We also found that the dissolved oxygen level was a critical parameter for β -ionone biosynthesis. This work should advance the potential of *Y. lipolytica* as a cell factory platform for the high-level production of terpenoids.

Results

Re-casting the β -ionone biosynthesis into three modules and the choice of *Y. lipolytica* strain

The overall pathway from glucose to β -ionone was organized into the following three modules, considering the two most important intermediates: acetyl-CoA and geranylgeranyl diphosphate (GGPP) [31–33] (Fig. 1a, b). (1) Module 1 (the cytosolic acetyl-CoA supply module): from glucose to acetyl-CoA; in this module, the metabolic flux from F6P to acetyl-CoA was rewired by the introduction of the two genes of the PK–PTA pathway [34]. (2) Module 2 (the MVA module): from acetyl-CoA to GGPP. (3) Module 3 (the β -ionone synthesis module): from GGPP to β -ionone. These modules were further divided into seven units for integration with DNA sizes ranging from 7.5 to 14.5 kb (Table 1). For the *Y. lipolytica*

strain, we knocked out the *ku70* and *ku80* genes of *Y. lipolytica* Po1f, to generate strain YLBI0003, in order to improve the homologous recombination (HR) efficiency, as previously reported [28, 35, 36] (Additional file 1: Fig. S1). Three modules were then successively integrated into strain YLBI0003 by reiterative recombination via the single plasmid CRISPR–Cas9-mediated genome editing system based on pCAS1yl [28], in the following order: modules 3, 2, 1.

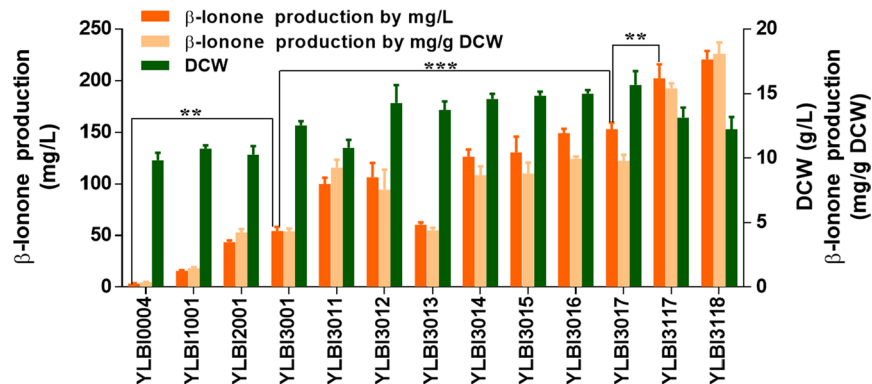
Enhancing the MVA module

The β -ionone synthesis module (Module 3) was first inserted into the *rDNA* locus of strain YLBI0003, the generated strain was designated as the baseline strain YLBI0004. In this module, the genes *carB*, *carRP* and *CCD1* were placed under the strong constitutive promoters P_{TEF1} , P_{EXPI} and P_{GPD2} , respectively. This strain only yielded 3.5 ± 0.2 mg/L β -ionone when cultured in YPD medium at 20 °C for 12 days (Additional file 1: Fig. S2a). Although the strain yielded a slightly higher β -ionone titer when the fermentation temperature was set at 15 °C, the higher cost of maintaining cultures at low temperature made us opt for 20 °C as the fermentation temperature during the optimization steps (Additional file 1: Fig. S2b).

Module 2, which controls the transformation of acetyl-CoA to GGPP, contains nine genes. Among them, two key genes hydroxymethylglutaryl-CoA reductase (*HMGRI*) and geranylgeranyl diphosphate synthase (*GGSI*) were singularly overexpressed or co-overexpressed in strain YLBI0004 under the control of P_{EXPI} and P_{TEF1} , respectively [36, 37]. For *HMGRI*, we used a truncated variant (*tHMGRI*) lacking the first 500 amino acid residues at the N-terminus, which was found to be more stable in the cytoplasm [37]. The strain YLBI3001, which overexpressed both *tHMG1* and *GGSI* genes, produced more β -ionone than the strains overexpressing only one of them (Fig. 2). This strain accumulated 54.2 ± 4.0 mg/L (4.3 ± 0.2 mg/g DCW) β -ionone, representing a 15-fold increase compared to the baseline strain YLBI0004.

Table 1 The modules and units constructed in this work

| Module | Unit | Name | Length/bp | Locus (first copy) | Locus (multi copy) |
|--------|------|------------------|-----------|--------------------|---------------------------|
| 1 | 1 | bbPK-bsPTA | 11,234 | <i>rDNA</i> | <i>pox4</i> , <i>xpr2</i> |
| 2 | 2 | ERG10-ERG13 | 11,451 | <i>lip1</i> | |
| | 3 | tHMG1 | 8820 | <i>D17</i> | |
| | 4 | ERG8-ERG12-ERG19 | 13,425 | <i>pox5</i> | |
| | 5 | IDI-ERG20 | 10,044 | <i>pox3</i> | |
| | 6 | GGSI | 7527 | <i>ku80</i> | |
| | 7 | carB-carRP-CCD1 | 14,440 | <i>rDNA</i> | <i>ku70</i> |



| | | | | | | | | | | | | | |
|----------|------------------|---|---|---|---|---|---|---|---|---|---|---|---|
| Module 3 | carB-carRP-CCD1 | • | • | • | • | • | • | • | • | • | • | • | • |
| Module 2 | GG51 | | • | | • | • | • | • | • | • | • | • | • |
| | tHMG1 | | | • | • | • | • | • | • | • | • | • | • |
| | ERG10+ERG13 | | | | • | | | • | • | | • | • | • |
| | IDI+ERG20 | | | | | • | | • | | • | • | • | • |
| | ERG8+ERG12+ERG19 | | | | | | • | | • | • | • | • | • |
| Module 1 | bbPK-bsPTA | | | | | | | | | | • | • | |

Fig. 2 β-ionone production in different engineered strains. Data represent the mean ± standard deviation (n = 3). Significance was marked by t-test, **p-value ≤ 0.01; ***p-value ≤ 0.001

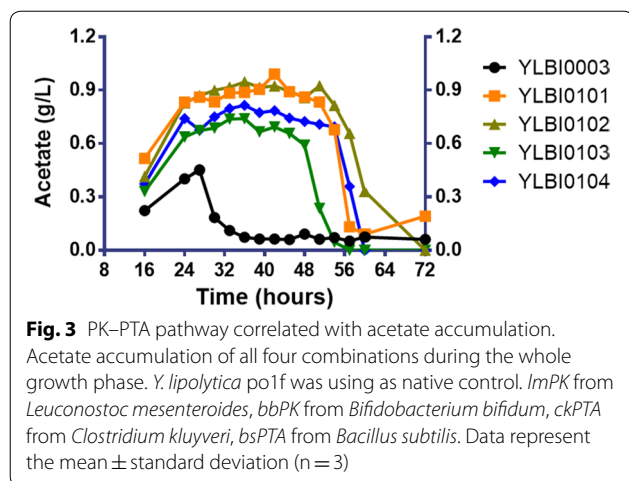
To further push the carbon flux from acetyl-CoA to β-ionone, the other three units containing 7 genes, *ERG10* (YALIOE11099g), *ERG13* (YALIOF30481g), *ERG8* (YALIOE06193g), *ERG12* (YALIOB16038g), *ERG19* (YALIOF05632g), *IDI* (YALIOF04015g), and *ERG20* (YALIOE05753g) were sequentially integrated downstream of native constitutive strong promoters (P_{TEFI} , P_{EXPI} or P_{GPD2}) into strain YLBI3001 (Fig. 1). Different integration combinations of the three units were investigated, and the strain harboring all three units (YLBI3017) showed the highest β-ionone titer of 152.9 ± 5.8 mg/L (9.8 ± 0.5 mg/g DCW). Therefore, overexpression of the whole Module 2 achieved a 43.7-fold increase in β-ionone yield compared to the baseline strain YLBI0004, or a 2.8-fold increase over the strain YLBI3001.

Enhancing the cytosolic acetyl-CoA supply by introduction of the PK-PTA pathway genes

In strain YLBI3017, the genes of Module 2 and 3 were overexpressed in cytoplasm, while the precursor acetyl-CoA was generated in the mitochondria, shuttled to the cytoplasm as citrate, and then converted to acetyl-CoA by acetyl-CoA synthetase. By this native pathway of cytosolic acetyl-CoA generation from glucose, there are as much as 14 steps that only a maximum of 2 mol of acetyl-CoA can be produced from 1 mol of glucose with 2 mol of carbon loss. The recently reported

PK-PTA pathway, a non-oxidative glycolytic pathway which consists of phosphoketolase (PK) and phosphotransacetylase (PTA), can yield a maximum of 3 mol of acetyl-CoA directly in the cytoplasm from 1 mol of glucose, with only four steps [34]. This pathway was successfully introduced into *Y. lipolytica* to yield a 16.4% increase of lipid titer [38].

In this work, two heterologous PKs under the control of P_{GPD2} (*ImpPK* from *Leuconostoc mesenteroides*; *bbPK* from *Bifidobacterium bifidum*) and two heterologous PTAs under the control of P_{TEFI} (*ckPTA* from *Clostridium kluyveri*; *bsPTA* from *Bacillus subtilis*) were assembled resulting in four combinations, and were first investigated separately using the baseline strain YLBI0003. As a metabolic intermediate, acetyl-CoA is rapidly depleted in the cytoplasm, therefore acetate, a derivative of acetyl-CoA, was used as the indicator for the production of acetyl-CoA [34]. The highest acetate titers in the strains containing *bbPK-bsPTA*, *bbPK-ckPTA*, *ImpPK-bsPTA* and *ImpPK-ckPTA* were 0.99 g/L, 0.95 g/L, 0.74 g/L and 0.81 g/L, respectively, representing titers significantly higher than that measured in the baseline strain YLBI0003 (0.45 g/L) (Fig. 3). Based on the hypothesis that the higher acetate production reflected a higher acetyl-CoA supply, *bbPK-bsPTA* was selected for further analysis. Moreover, we found that the overexpression of the PK-PTA pathway also enhanced the growth



of *Y. lipolytica* (Additional file 1: Fig. S3), in contrast to previous results [34].

The *bbPK-bsPTA* was then further evaluated for the effect of different integration loci and copy numbers of PK-PTA pathway, but this time on the basis of strain YLBI3001 that overexpressed *tHMG1* and *GGSI* in addition to Module 3 (Additional file 1: Fig. S4a). The β -ionone titer improved 2.04-fold, 1.93-fold and 2.50-fold (110.3 ± 4.6 mg/L, 104.5 ± 4.5 mg/L and 135.4 ± 3.8 mg/L) when *bbPK-bsPTA* was inserted at *rDNA*, *pox4* and *xpr2* loci, respectively (Additional file 1: Fig. S5). However, the increase of *bbPK-bsPTA* copy number reduced the titer of β -ionone while promoting the cell growth (Additional file 1: Fig. S5). Thus, subsequently, a copy of *bbPK-bsPTA* was integrated at the *xpr2* locus of strain YLBI3017 to generate strain YLBI3117 that harboring all the three modules. The strain YLBI3117 showed a 32% higher β -ionone production than strain YLBI3017 (202.2 ± 13.6 mg/L, 15.4 ± 0.4 mg/g DCW) (Fig. 2).

It was found that 118.8 ± 18.1 mg/L (14.5 ± 3.0 mg/g DCW) β -carotene accumulated in strain YLBI3117 (Additional file 1: Fig. S4b). We thus considered to increase the copy number of Module 3 to improve the production of β -ionone from GGPP. Thus, another copy of Module 3 was integrated at *ku70* locus of strain YLBI3117 to generate strain YLBI3118, but only a slight increase (9%) of β -ionone yield was achieved (Fig. 2). This final strain produced 220.7 ± 8.0 mg/L (18.1 ± 0.9 mg/g DCW) β -ionone in 12 days of shake-flask fermentation while at day 3, day 6 and day 9, the yields were 50.0 ± 3.9 mg/L, 132.1 ± 5.8 mg/L and 154.0 ± 15.7 mg/L, respectively. (Additional file 1: Fig. S6a, b).

Since the final strain YLBI3118 was still *leu* defective, the *leu* gene was then complemented to generate strain YLBI3119. This resulted in an 89% increase in biomass

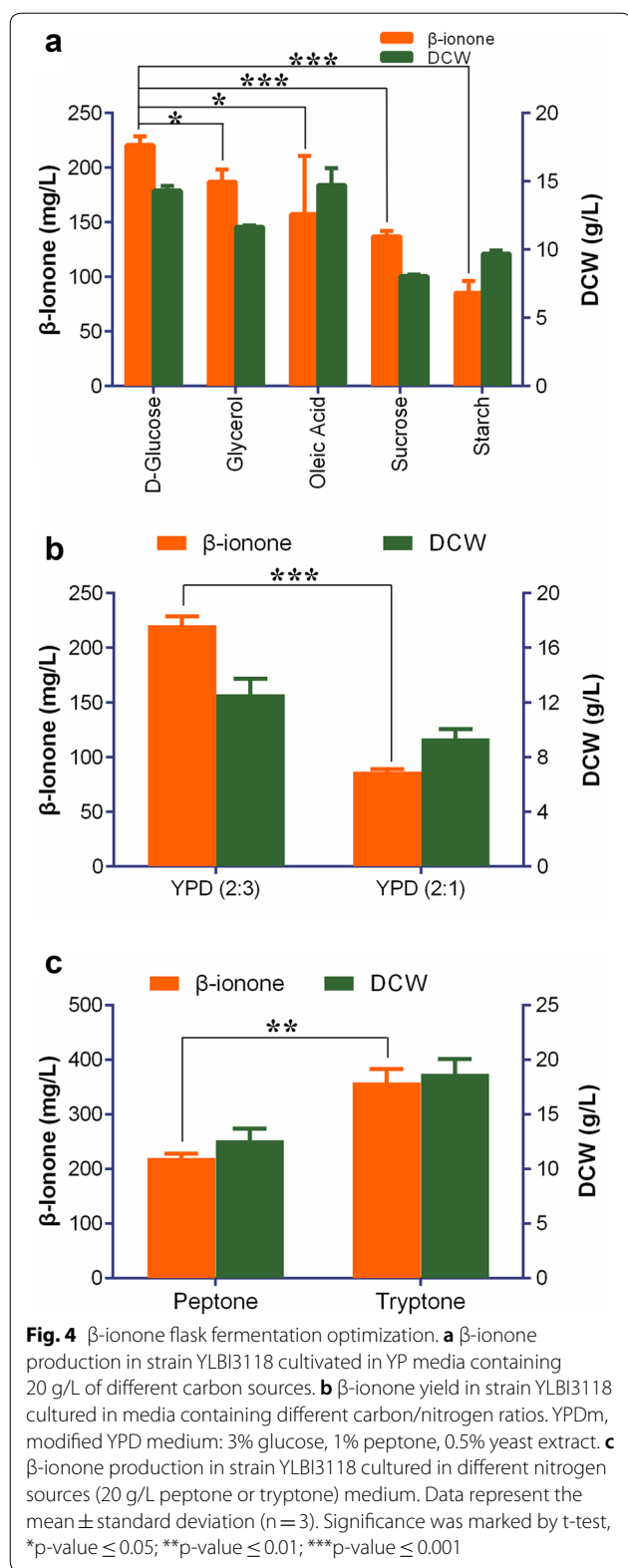
(Additional file 1: Fig. S7). While there was no significant difference in the β -ionone yield (p -value = 0.35) on the basis of volume, however, the yield on the basis of cell mass (mg/g DCW) was significantly reduced from 19.2 ± 2.5 to 10.8 ± 0.5 mg/g DCW.

High-level production of β -ionone in fed-batch fermentation

Before using the bioreactor fermentation, we investigated the effect of carbon sources and nitrogen sources on the β -ionone production in shake-flasks. 20 g/L of glycerol, starch, sucrose and oleic acid were used to replace glucose for the yeast fermentation, respectively. Although glycerol and oleic acid are commonly regarded as the optimal carbon sources for organic acids or terpenoids production in *Y. lipolytica* [30, 37], we found that glucose was the best carbon source in this case (Fig. 4a). It is likely because for this engineered strain, a maximum of 3 mol of acetyl-CoA could be produced from 1 mol of glucose via the PK-PTA pathway [34] (Fig. 1a), while only a maximum of 1 mol of acetyl-CoA could be produced from 1 mol of glycerol by the glycolysis and the tricarboxylic acid cycle pathways [39]. Moreover, *Y. lipolytica* lacks efficient endogenous enzymes for utilization of sucrose or starch [39, 40]. On the other hand, while 1 mol of oleic acid could yield a maximum of 9 mol of acetyl-CoA, in *Y. lipolytica* oleic acid appears to be utilized more for lipid accumulation [41].

It was reported that nitrogen limitation was favorable for the accumulation of carotenoids [37]. However, we obtained only 86.8 ± 2.5 mg/L (9.3 ± 0.6 mg/g DCW) β -ionone when the amount of nitrogen source (yeast extract and peptone) was reduced according to the carbon to nitrogen (C/N) ratio from 2:3 to 2:1 (wt/wt) (Fig. 4b). This indicates that a rich nitrogen supplement is an important parameter for β -ionone production in strain YLBI3118. Furthermore, the change of peptone with tryptone as the nitrogen source dramatically increased the β -ionone titer up to 358.4 ± 25.0 mg/L (19.2 ± 2.5 mg/g DCW) (Fig. 4c). It should be noted that the β -ionone titer was only calculated from the organic phase, as β -ionone was undetectable in the aqueous medium and was detected only at low concentrations (< 10 mg/L culture) in the cell pellets (data not shown).

To further enhance β -ionone production, the fermentation of strain YLBI3118 was performed in 3-L bioreactor. In a first test we observed a long lag phase probably caused by the high-concentration medium used (100 g/L glucose, 50 g/L tryptone, 20 g/L yeast extract), and the titer of β -ionone was only 148 mg/L, much lower than that obtained in shake-flask fermentation (Additional file 1: Fig. S8). In the following test the fermentation was started in $1 \times$ YPD medium, then after



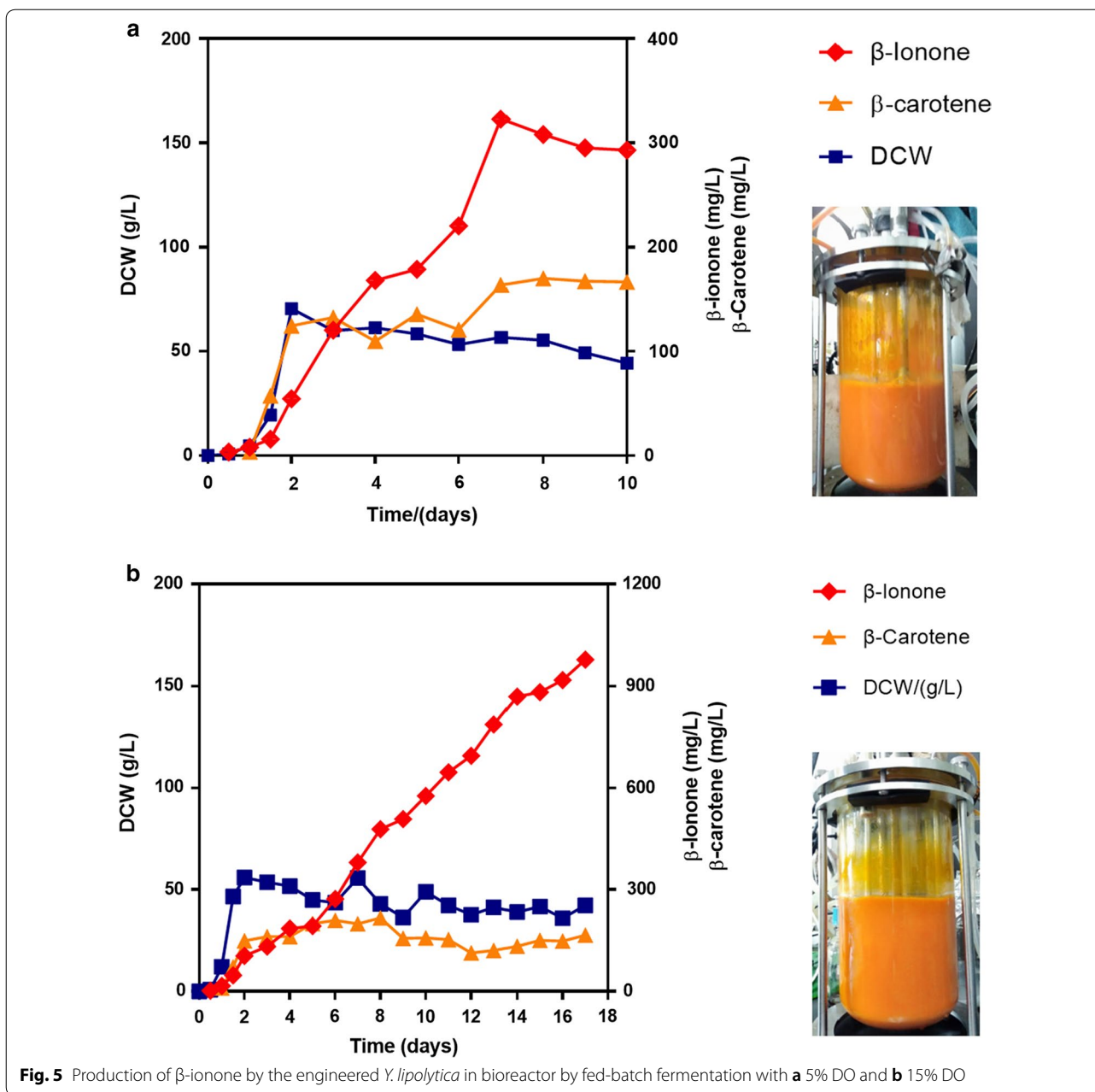
12 h of fermentation the medium was fed with 250 mL 10 \times YPDm supplied at 0.4 mL/min, followed by 600 g/L

glucose supplied at 0.1 mL/min. In this batch, the dissolved oxygen (DO) dropped to 0–5% at 12 h till the end of the fermentation. After 7 days (168 h) of fermentation, although the β -ionone productivity increased from 1.2 to 1.9 mg/L/h, the yield resulted 322 mg/L, still lower than that obtained in shake-flask fermentation (Fig. 5a). We speculated that the activity of the dioxygenase CCD1, which converts β -carotene to β -ionone, was limited by the low DO (0–5%). Thus, a series of fed-batch fermentations were conducted by setting the DO to 15%, 25% and 35%. The highest titer of β -ionone (0.98 g/L) was obtained after 17 days (408 h) of fermentation with the DO set at 15% (Fig. 5b). The further increase of DO to 25% and 35% was detrimental to the β -ionone production, and only 0.55 g/L and 0.40 g/L β -ionone were obtained in these conditions, respectively (Additional file 1: Fig. S9a, b). In summary, strain YLB13118, which was engineered by modular pathway engineering for the overproduction of β -ionone, when cultured the fed-batch fermentation at the optimum DO of 15% in 3-L bioreactor, produced 0.98 g/L β -ionone, which, to the best of our knowledge, is the highest yield of β -ionone obtained in cell factories to date.

Discussion

A rapidly increasing number of microbial cell factories have been constructed for the biosynthesis of natural products. Two main aspects are important for the application of these cell factories for commercial purposes: the product should be in high yield and regarded as natural. For these reasons, *Y. lipolytica*, a GRAS strain, has attracted great attention in recent years, especially for the production of terpenoids. Several useful synthetic biology tools have been aiding the creation of new and better performing *Y. lipolytica* strains [42, 43]. To date, the highest yields of lipid, lycopene and carotene produced via microbial cell factories have been achieved by using engineered *Y. lipolytica* strains [7, 12].

In this study, a modular pathway engineering method was used to promote the β -ionone production in *Y. lipolytica* (Fig. 1a, Additional file 1: Fig. S10). First, the integration of Module 3 yielded a low concentration of β -ionone. Then, the integration of Module 2 resulted in a 43.7-fold increase of the β -ionone titer. On the basis of this, Module 1 led to a 1.3-fold increase, and another copy of Module 3 led to a 1.1-fold increase, of β -ionone production. Finally, the fermentation optimization achieved a 4.4-fold increase in the titer, or 0.98 g/L of β -ionone. This is significantly higher than the previously reported titer of 380 mg/L [30], although the β -ionone productivity (2.4 mg/L/h) is lower than those of previous studies, e.g. 10 mg/L/h in *E. coli* [23], 2.5 mg/L/h in *S. cerevisiae* [44] and 2.7 mg/L/h in *Y. lipolytica* [30]



(Additional file 2: Table S1). Additionally, while our fermentation yields were slightly lower than those obtained in the previous work at similar fermentation intervals [30] (e.g. flask: 50 mg/L at day 3 vs. 68 mg/L at day 4; bioreactor: 272 mg/L at day 6 vs. 380 mg/L at day 6), the β -ionone titer was notably increased to 358 mg/L after 12 days of flask fermentation in the optimized conditions, and 0.98 g/L after 17 days of bioreactor fermentation. This indicates that the extension of fermentation time is favorable for the accumulation of β -ionone.

Within the Module 2, *tHMG1* is considered a major rate-limiting enzyme [36]. In our work, the titer of β -ionone increased 13-fold in the strain that overexpressed *tHMG1*. This is consistent with a previous report showing that the β -carotene titer increased 3.4-fold when *tHMG1* was overexpressed [18]. As a future perspective, the integration of multiple copies of *tHMG1* and other MVA related genes could be considered to further increase the flux of MVA pathway [36].

Our study confirmed that the introduction of PK-PTA pathway is a useful route to increase terpenoids

production by increasing the production of acetyl-CoA directly in the cytosol. As *Y. lipolytica* is recognized to have a unique propensity for high flux through acetyl-CoA, several groups have focused on using the PK–PTA pathway for the improvement of the synthesis of acetyl-CoA derivatives such as lipid and triacetic acid lactone [4, 30, 32, 45]. To the best of our knowledge, this work is the first that uses the PK–PTA pathway to increase terpenoids production in *Y. lipolytica*.

In the fermentation optimization, we found that a medium rich in nitrogen sources is the optimal choice to achieve the best performance. This result is in sharp contrast to the results obtained for the biosynthesis of β -carotene, which showed an opposite trend [36]. It could be due to that the nitrogen limitation is favorable for the accumulation of lipid bodies and therefore promotes the accumulation of β -carotene which resides in lipid bodies in *Y. lipolytica* [36, 37], while in our case, the β -ionone was transported to the extracellular and enriched in the dodecane. Also, consistent with a previous report in which tryptone was found to improve the production of acetyl-CoA, and to promote the biosynthesis of acetyl-CoA-derived products [46], the β -ionone titer increased 62% when tryptone was used in place of peptone in shake-flask fermentation.

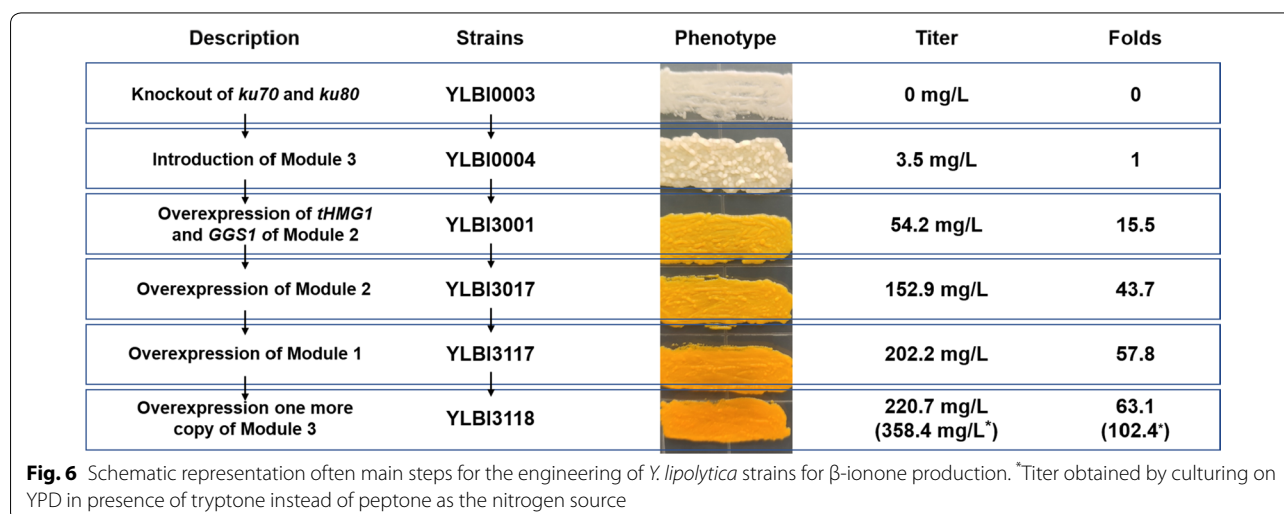
In the subsequent 3-L bioreactor fermentation, it was found that the DO was a very important factor for the biosynthesis of β -ionone. This is consistent with a recent report [47] and is related to the last metabolic step of β -ionone biosynthesis, which is catalyzed by carotenoid cleavage dioxygenase and requires two oxygen molecules to produce two β -ionone molecules. Thus, with the optimization of DO level at 15% the yield of β -ionone increased twofold compared to the bioreactor fermentation performed with DO at 0–5%. As another future

perspective, one effective strategy to enhance the biosynthesis of β -ionone could be the introduction of a more powerful CCD1 enzyme to improve the specific cleavage of β -carotene [30]. In another report, protein engineering was performed to improve the membrane affinity of *PhCCD1*, which was derived from *Petunia hybrida*, and 184 mg/L β -ionone was produced in *S. cerevisiae* at the end of 3 days flask fermentation [44]. Thus, the enzyme engineering of CCD1 was an alternative workable method to improve β -ionone biosynthesis.

Here, *Y. lipolytica* was engineered to become a cell factory and yield the highest β -ionone titer reported to date (Fig. 6). By replacing the relevant genes, the engineered strains could also be adapted for the biosynthesis of many other terpenoids based on the MVA pathway such as taxol [48], artemisinin [49], cannabinoid [50] and many others.

Conclusions

The GRAS yeast *Y. lipolytica* is an emerging microorganism platform for the production of natural terpenoids and their derivatives. In this work, we used a modular pathway engineering approach based on a set of modules and units for the facile and effective construction of *Y. lipolytica* microbial cell factories for the high-level production of β -ionone. Three modules were responsible for the enhancement of cytosolic acetyl-CoA supply through the PK–PTA pathway, the increase of MVA pathway flux and the synthesis of β -ionone. By the optimization of the design of the three modules, the carbon sources, the nitrogen level and the dissolved oxygen level, the highest titer of 0.98 g/L β -ionone was achieved in a 3-L fermenter by fed-batch fermentation.



Methods

Strains, media and culture condition

Escherichia coli DH5 α was used for cloning and plasmid construction. *E. coli* DH5 α was cultured in lysogeny broth (LB, 10 g/L tryptone, 5 g/L yeast extract, and 10 g/L NaCl) supplemented with 50 mg/mL ampicillin at 37 °C under constant shaking. *Y. lipolytica* Po1f (*MatA*, *leu2-270*, *ura3-302*, *xpr2-322*, *axp1-2* *Leu*⁻, *Ura*⁻, *DAEP*, *DAXP*, *Suc*⁺) was a kind gift from Dr. Catherine Madzak [39]. *Y. lipolytica* strains were cultured in yeast extract peptone dextrose (YPD) medium (10 g/L yeast extract, 20 g/L peptone, 20 g/L glucose) or in modified YPD medium (YPDm, 10 g/L yeast extract, 20 g/L tryptone, 20 g/L glucose). The low nitrogen content YPD contained 5 g/L yeast extract, 10 g/L tryptone, 30 g/L glucose. Synthetic dextrose medium lacking uracil and leucine (SD/(-Leu/-Ura)), 6.7 g/L yeast nitrogen base without amino acids, 0.62 g/L dropout supplement lacking leucine, tryptophan and uracil (DO/(-Leu/-Trp/-Ura)), 20 g/L glucose, 5 g/L (NH₄)₂SO₄, supplemented with 100 mg/L tryptophan) was used for the selection of the integrated strains containing the assembled biochemical pathway. Synthetic dextrose medium lacking uracil (SD/-Ura) was obtained by adding 20 mg/L leucine and 100 mg/L tryptophan to the SD/(-Leu/-Trp/-Ura) medium. For the optimization of carbon sources, the yeast extract peptone (YP) medium (10 g/L yeast extract, 20 g/L peptone) was supplemented with 20 g/L glycerol or soluble starch or sucrose or oleic acid. During the construction the yeast strains were incubated at 30 °C under shaking (250 rpm). For plate cultivation, 2% agar was added to the culture medium. For β -ionone fermentation, the yeast strains were cultured in 50-mL shake-flasks containing 20 mL YPD medium and 10% (v/v) of dodecane at 20 °C, under shaking at 250 rpm.

Construction of plasmids and strains

All the plasmids are listed in Table 2. The primers used for the construction of these plasmids are listed in Additional file 2: Table S2. The original CRISPR–Cas9 mediated genome editing plasmid pCAS1yl was a kind gift from Prof. Sheng Yang [28]. The 20-nt sequence at the 5'-end of the gRNA was modified for the gene unit integration by using the oligo DNA listed in Additional file 2: Table S2. The sequences of *carB* and *carRP* genes from *Mucor circinelloides* [36] and the sequence of *PhCCDI* gene from *Petunia hybrida* [51] were codon-usage optimized and synthesized by Sangon Biotech Co. Ltd. (Shanghai, China). All the homologous arms, promoters, terminators and endogenous genes were amplified from *Y. lipolytica* genomic DNA. Three endogenous promoters (*P_{TEF1}*, *P_{EXP1}*, *P_{GPD2}*) were separately used in this work. All the seven integration units (Fig. 1b) were flanked by

two 600–1100 bp homologous arms. The selection maker cassette hisG-Ura3-hisG (HUH), which was a kind gift from Prof. Sheng Yang [36], was used for gene unit integration. The DNA fragments were assembled by Gibson assembly [27]. *Not* I digested sites were used for the linearization of the units. The transformation of the plasmids and the linear DNA fragments into *Y. lipolytica* was performed using the Frozen-EZ Yeast Transformation II kit (Zymo Research Corporation). The transformation mix was spread on the selection plate and *Y. lipolytica* was cultured at 30 °C for 4 days. Detailed information for the plasmid construction is shown in Additional file 3.

To generate *Y. lipolytica* Po1f($\Delta ku70\Delta ku80$), named YLBI0003 in this study, two CRISPR/Cas9 plasmids targeting *ku70* and *ku80* genes, respectively, were co-transformed with corresponding homologous arm fragments into *Y. lipolytica* Po1f. Eight gene loci (*rDNA*, *pox3*, *pox5*, *lip1*, *D17*, *xpr2*, *ku70* and *ku80*) of the genome were selected for the integration of these units [52–54]. The Module 3 (the β -ionone synthesis module) was first integrated at the *rDNA* locus of strain YLBI0003 to generate strain YLBI0004. Five units of the Module 2 (the MVA module) including 9 endogenous genes (*ERG10*+*ERG13*, *tHMG1*, *ERG8*+*ERG12*+*ERG19*, *IDI*+*ERG20* and *GGS1*) were then integrated into five loci (*lip1*, *D17*, *pox5*, *pox3* and *ku80*) of YLBI0004 with different unit combinations (Fig. 1a). The Module 1 (the acetyl-CoA supply module) was subsequently integrated into the *xpr2* locus of strain YLBI3017 to generate strain YLBI3117. Another copy of Module 3 was also integrated at the *ku70* locus of strain YLBI3117 to generate strain YLBI3118. All the strains constructed in this study are listed in Table 3. KOD FX DNA polymerase (Toyobo Co; Osaka, Japan) was used for colony PCR to confirm the strain genotypes using the primers listed in Additional file 2: Table S3. The PCR products were sequenced at Sangon Biotech Co. Ltd. (Shanghai, China). The pCAS1yl-gRNA plasmid was simply cured by picking out the single colonies followed by culturing in YPD medium for about 16 h until the OD₆₀₀ was approximately 3 and then plating onto YPD agar with a 1000-fold dilution. The Ura3 selection maker was cured by incubating the strain on YPD plate containing 1 mg/mL 5-fluoroorotic acid for 2–3 days. The larger colonies were then streaked onto SD and SD/-Ura plates and were cultured at 30 °C for 2 more days.

Integration verification

All the primers for colony PCR verification are listed in Additional file 2: Table S3. Briefly, the *ku70* and *ku80* knockout strains were confirmed by colony PCR using the *ku70*-CP-F/R and *ku80*-CP-F/R primer pairs. The strain integrated with the Module 3 for the β -ionone synthesis was first picked out based on the yellow phenotype

Table 2 The plasmids used in this work

| Name | Relative characteristics | Source |
|-------------------------------|--|-----------|
| pUC19 | | TaKaRa |
| pTAs-HUH | <i>HisG-Ura3-HisG</i> maker recycled cassette | [36] |
| pCAS1yl | <i>TRP1</i> Guide RNA module and Cas9 expression cassette in pMCSCen1 | [36] |
| pCAS1yl-ku70 | <i>Ku70</i> Guide RNA module and Cas9 expression cassette in pMCSCen1 | This work |
| pCAS1yl-ku80 | <i>Ku80</i> Guide RNA module and Cas9 expression cassette in pMCSCen1 | This work |
| pCAS1yl-rDNA | <i>rDNA</i> Guide RNA module and Cas9 expression cassette in pMCSCen1 | This work |
| pCAS1yl-D17 | <i>D17</i> Guide RNA module and Cas9 expression cassette in pMCSCen1 | This work |
| pCAS1yl-lip1 | <i>Lip1</i> Guide RNA module and Cas9 expression cassette in pMCSCen1 | This work |
| pCAS1yl-pox3 | <i>Pox3</i> Guide RNA module and Cas9 expression cassette in pMCSCen1 | This work |
| pCAS1yl-pox4 | <i>Pox4</i> Guide RNA module and Cas9 expression cassette in pMCSCen1 | This work |
| pCAS1yl-pox5 | <i>Pox5</i> Guide RNA module and Cas9 expression cassette in pMCSCen1 | This work |
| pCAS1yl-LEU2 | <i>LEU2</i> Guide RNA module and Cas9 expression cassette in pMCSCen1 | This work |
| pCAS1yl-XPR2 | <i>XPR2</i> Guide RNA module and Cas9 expression cassette in pMCSCen1 | This work |
| pUC19-TBX | P_{TEF1} - <i>CarB-xpr2t</i> cassette in pUC19 | This work |
| pUC19-ERPL | P_{EXP1} - <i>CarRP-lip2t</i> cassette in pUC19 | This work |
| pUC19-GCM | P_{GPD2} - <i>CCD1-mig1t</i> cassette in pUC19 | This work |
| pUC19-TGX | P_{TEF1} - <i>GG51-xpr2t</i> cassette in pUC19 | This work |
| pUC19-GTM | P_{EXP1} - <i>tHMG1-lip2t</i> cassette in pUC19 | This work |
| pUC19-rDNA-BPC | P_{TEF1} - <i>CarB-xpr2t</i> and P_{EXP1} - <i>CarRP-lip2t</i> and P_{GPD2} - <i>CCD1-mig1t</i> cassettes in pUC19-rDNA-HUH | This work |
| pUC19-ku70-BPC | P_{TEF1} - <i>CarB-xpr2t</i> and P_{EXP1} - <i>CarRP-lip2t</i> and P_{GPD2} - <i>CCD1-mig1t</i> cassettes in pUC19-ku70-HUH | This work |
| pUC19-ku80-GGS1-HUH | P_{TEF1} - <i>GG51-xpr2t</i> cassette in pUC19-ku80-HUH | This work |
| pUC19-D17-tHMG1-HUH | P_{EXP1} - <i>tHMG1-lip2t</i> cassette in pUC19-D17-HUH | This work |
| pUC19-lip1-ERG10ERG13-HUH | P_{TEF1} - <i>ERG10-erg10t</i> and P_{GPD2} - <i>ERG13-erg13t</i> cassettes in pUC19-lip1-HUH | This work |
| pUC19-POX3-IDIERG20-HUH | P_{EXP1} - <i>IDI-ident</i> and P_{TEF1} - <i>ERG20-erg20t</i> cassettes in pUC19-pox3-HUH | This work |
| pUC19-POX5-ERG8ERG12ERG19-HUH | P_{EXP1} - <i>ERG8-erg8t</i> , P_{TEF1} - <i>ERG12-erg12t</i> and P_{GPD2} - <i>ERG19-erg19t</i> cassettes in pUC19-pox5-HUH | This work |
| pUC19-rDNA-BB-PK-PTA-HUH | P_{GPD2} - <i>B. b pk-mig1t-P_{TEF1}-B. s pta-xpr2t</i> cassettes in pUC19-rDNA-HUH | This work |
| pUC19-rDNA-BC-PK-PTA-HUH | P_{GPD2} - <i>B. b pk-mig1t-P_{TEF1}-C. k pta-xpr2t</i> cassettes in pUC19-rDNA-HUH | This work |
| pUC19-rDNA-LB-PK-PTA-HUH | P_{GPD2} - <i>L. m pk-mig1t-P_{TEF1}-B. s pta-xpr2t</i> cassettes in pUC19-rDNA-HUH | This work |
| pUC19-rDNA-LC-PK-PTA-HUH | P_{GPD2} - <i>L. m pk-mig1t-P_{TEF1}-C. k pta-xpr2t</i> cassettes in pUC19-rDNA-HUH | This work |
| pUC19-POX4-BB-PK-PTA-HUH | P_{GPD2} - <i>B. b pk-mig1t-P_{TEF1}-B. s pta-xpr2t</i> cassettes in pUC19-POX4-HUH | This work |
| pUC19-XPR2-BB-PK-PTA-HUH | P_{GPD2} - <i>B. b pk-mig1t-P_{TEF1}-B. s pta-xpr2t</i> cassettes in pUC19-XPR2-HUH | This work |

Other plasmids can be found in Additional file 3

and the genotype was verified by PCR using *CarB-CP-F/R*, *CarRP-CP-F/R* and *CCD1-CP-F/R* primer pairs. All the other integrated strains were confirmed with the relevant primers. The PCR products were sequenced at Sangon Biotech Co. Ltd. (Shanghai, China). Real-time qPCR was performed to determine the copy number of the inserted units using the TB Green™ Premix Ex Taq™ kit (TaKaRa, Dalian, China). The PCR reaction was monitored on an ABI 7500 real Time PCR System. The *act1* homologous genes were chosen as reference.

Fed-batch fermentations in 3-L bioreactor

The initial fermentation was completed using 1.2 L YPDM medium containing 20 g/L glucose, 20 g/L tryptone, 10 g/L yeast extract in 3-L bioreactor (BioFlo/

CelliGen 115, New Brunswick, Canada). The seed culture was incubated in a shake-flask at 30 °C, 250 rpm for 16 h and inoculated into the bioreactor at an initial OD~0.2. Dodecane (150 mL, 10% v/v) was used as the initial organic overlay layer. 250 mL 10× YPDM was fed at 0.4 mL/min after 12 h fermentation, followed by 600 g/L glucose at 0.1 mL/min till the end of the fermentation. The temperature was maintained at 20 °C throughout the fermentation. The pH was maintained at 5.5 by the automatic addition of 3 M NaOH or 3 M HCl. The dissolved oxygen (DO) was set at 0–5%, 15%, 25%, 35% under automatic control of agitation speed (100–1000 rpm), and the aeration was set at 2 L/min. Pure oxygen gas was essential to achieve high DOs.

Table 3 *Y. lipolytica* strains constructed in this work

| strains | Characteristics | Source |
|---------------|---|-----------|
| CLIB 724/po1f | <i>MatA, leu2-270, ura3-302, xpr2-322, axp1-2 Leu-, Ura-, DAEP, DAXP, Suc+</i> | [39] |
| YLBI0001 | CLIB 724 $\Delta ku70::hisG$ | This work |
| YLBI0002 | CLIB 724 $\Delta ku80::hisG$ | This work |
| YLBI0003 | YLBI0001 $\Delta ku80::hisG$ | This work |
| YLBI0004 | YLBI0003 $\Delta rDNA::P_{TEF1}-CarB-xpr2t, P_{EXP1}-CarRP-lip2t, P_{GPD2}-CCD1-mig1t$ | This work |
| YLBI1001 | YLBI0004 $\Delta KU80::P_{TEF1}-GG51-xpr2t$ | This work |
| YLBI2001 | YLBI0004 $\Delta D17::P_{EXP1}-tHMG1-lip2t$ | This work |
| YLBI3001 | YLBI1001 $\Delta D17::P_{EXP1}-tHMG1-lip2t$ | This work |
| YLBI3011 | YLBI3001 $\Delta lip1::P_{TEF1}-ERG10-erg10t, P_{GPD2}-ERG13-erg13t$ | This work |
| YLBI3012 | YLBI3001 $\Delta Pox3::P_{EXP1}-IDl-idit, P_{TEF1}-ERG20-erg20t$ | This work |
| YLBI3013 | YLBI3001 $\Delta Pox5::P_{EXP1}-ERG8-erg8t, P_{TEF1}-ERG12-erg12t, P_{GPD2}-ERG19-erg19t$ | This work |
| YLBI3014 | YLBI3011 $\Delta Pox3::P_{EXP1}-IDl-idit, P_{TEF1}-ERG20-erg20t$ | This work |
| YLBI3015 | YLBI3011 $\Delta Pox5::P_{EXP1}-ERG8-erg8t, P_{TEF1}-ERG12-erg12t, P_{GPD2}-ERG19-erg19t$ | This work |
| YLBI3016 | YLBI3012 $\Delta Pox5::P_{EXP1}-ERG8-erg8t, P_{TEF1}-ERG12-erg12t, P_{GPD2}-ERG19-erg19t$ | This work |
| YLBI3017 | YLBI3014 $\Delta Pox5::P_{EXP1}-ERG8-erg8t, P_{TEF1}-ERG12-erg12t, P_{GPD2}-ERG19-erg19t$ | This work |
| YLBI0101 | YLBI0003 $\Delta rDNA::P_{GPD2}-B. b pk-mig1t-P_{TEF1}-B. s pta-xpr2t$ | This work |
| YLBI0102 | YLBI0003 $\Delta rDNA::P_{GPD2}-B. b pk-mig1t-P_{TEF1}-C. k pta-xpr2t$ | This work |
| YLBI0103 | YLBI0003 $\Delta rDNA::P_{GPD2}-L. m pk-mig1t-P_{TEF1}-B. s pta-xpr2t$ | This work |
| YLBI0104 | YLBI0003 $\Delta rDNA::P_{GPD2}-L. m pk-mig1t-P_{TEF1}-C. k pta-xpr2t$ | This work |
| YLBI3110 | YLBI3001 $\Delta rDNA::P_{GPD2}-B. b pk-mig1t-P_{TEF1}-B. s pta-xpr2t$ | This work |
| YLBI3111 | YLBI3001 $\Delta POX4::P_{GPD2}-B. b pk-mig1t-P_{TEF1}-B. s pta-xpr2t$ | This work |
| YLBI3112 | YLBI3001 $\Delta XPR2::P_{GPD2}-B. b pk-mig1t-P_{TEF1}-B. s pta-xpr2t$ | This work |
| YLBI3113 | YLBI3111 $\Delta POX4::P_{GPD2}-B. b pk-mig1t-P_{TEF1}-B. s pta-xpr2t$ | This work |
| YLBI3114 | YLBI3111 $\Delta XPR2::P_{GPD2}-B. b pk-mig1t-P_{TEF1}-B. s pta-xpr2t$ | This work |
| YLBI3115 | YLBI3112 $\Delta XPR2::P_{GPD2}-B. b pk-mig1t-P_{TEF1}-B. s pta-xpr2t$ | This work |
| YLBI3116 | YLBI3113 $\Delta XPR2::P_{GPD2}-B. b pk-mig1t-P_{TEF1}-B. s pta-xpr2t$ | This work |
| YLBI3117 | YLBI3017 $\Delta rDNA::P_{GPD2}-B. b pk-mig1t-P_{TEF1}-B. s pta-xpr2t$ | This work |
| YLBI3118 | YLBI3117 $\Delta ku70::P_{TEF1}-CarB-xpr2t, P_{EXP1}-CarRP-lip2t, P_{GPD2}-CCD1-mig1t$ | This work |

Biomass, sugar and organic acid quantification

A 1 mL aliquot of cultured cells was harvested and dried at 60 °C for 48 h to measure the DCW. Acetate, glucose and other carbon sources were filtered by through 0.2 µm pore size membrane and then quantified by high-performance liquid chromatography (HPLC) using an Agilent1260 Infinity series system (Agilent Technologies, USA) equipped with an Aminex HPX 87H column (300 mm × 7.8 mm, Bio-Rad Laboratories, USA) and a refractive index detector set at 210 nm. The analytes were eluted with 5 mM H₂SO₄ at 60 °C at 0.6 mL/min flow rate.

β-ionone quantification

The organic phase was carefully pipetted from the culture sample and centrifuged for 5 min at 12,000 rpm. β-ionone in the aqueous medium and cell pellets were extracted using dodecane as described in literature [30]. The supernatant organic phase filtered by through 0.2 µm pore size membrane and analyzed by injecting a 1 µL sample into

a gas chromatography system HP 7890A (Agilent Technologies, USA) coupled to a flame ionization detector using a DB-FFAP capillary column (60 m × 0.25 mm id, 0.25 µm film thickness) (J&W Scientific, Agilent Technologies, USA). The oven program was set as follows: start at 80 °C for 1 min, then the temperature was raised up 10 °C/min to 120 °C and kept constant for 1 min then raised 10 °C/min to 240 °C. The standard curve was constructed within the range of 1 mg/L-100 mg/L β-ionone. Isolongifolene (Sigma-Aldrich, USA) was used as internal standard.

β-carotene quantification

For β-carotene extraction, 0.1 mL cultured cells were harvested by centrifugation for 5 min at 12,000 rpm. A 0.7 mL aliquot of dimethyl sulfoxide was used to resuspend the cells followed by an incubation at 55 °C for 10 min. After addition of 0.7 mL acetone, the sample was incubated at 45 °C for 15 min. The sample was centrifuged at 13,000g for 5 min. The supernatant was

filtered by through 0.2 μm pore size membrane and then analyzed by HPLC using an Agilent 1260 Infinity serious system (Agilent Technologies, USA) with an UV detector (wavelength 450 nm) and an XDB-C18 column (5 μm , 4.6×150 mm, Agilent Technologies, USA). The mobile phase consisted of methanol, acetonitrile and dichloromethane (42:42:16) with a flow rate of 1.0 mL/min at 30 $^{\circ}\text{C}$.

Supplementary information

Supplementary information accompanies this paper at <https://doi.org/10.1186/s12934-020-01309-0>.

Additional file 1: Figures S1–S10.

Additional file 2: Table S1–S3.

Additional file 3. Methods for plasmids construction.

Abbreviations

PK: Phosphoketolase; PTA: Phosphotransacetylase; ERG10: Acetoacetyl-CoA thiolase; ERG13: Hydroxymethylglutaryl-CoA synthase; tHMGR: Truncated hydroxymethylglutaryl-CoA reductase; ERG8: Phosphomevalonate kinase; ERG12: Mevalonate kinase; ERG19: Mevalonate diphosphate decarboxylase; IDI: Isopentenyl diphosphate isomerase; ERG20: Geranyl/farnesyl diphosphate synthase; GGS1: GGPP synthase; carB: Phytoene dehydrogenase; carRP: Phytoene synthase/lycopene cyclase; CCD1: Carotenoid cleavage dioxygenase; HMg-CoA: Hydroxymethylglutaryl-CoA; IPP: Isopentenyl diphosphate; DMAPP: Dimethylallyl diphosphate; FPP: Farnesyl diphosphate; GGPP: Geranylgeranyl diphosphate; *Y. lipolytica*: *Yarrowia lipolytica*; HR: Heterologous recombination; HUH: HisG-Ura3-HisG; YPD: Yeast extract-peptone-dextrose; DCW: Dry cell weight; DO: Dissolved oxygen; C/N: Ratio of carbon resource to nitrogen resource; HPLC: High-performance liquid chromatography.

Acknowledgements

We thank Prof. Sheng Yang (Key Laboratory of Synthetic Biology, CAS Center for Excellence in Molecular Plant Sciences, Institute of Plant Physiology and Ecology, Chinese Academy of Sciences, China) for providing us with plasmids pCAS1yl and pAT-HUH. We are also grateful to Dr. Catherine Madzak (GMPA, AgroParisTech, INRA, Université Paris-Saclay, France) and Prof. Qingsheng Qi (State Key Laboratory for Microbial Technology, Shandong University, China) for providing us with Po1f strain. We also thank Dr. Marco Pistozzi (School of Biology and Biological Engineering, South China University of Technology, China) for manuscript revision.

Authors' contributions

XFY and YPL participated in the design of the study. YPL and QYY performed the experimental work. YPL and XFY wrote the manuscript. XFY and ZLL conceived the study, supervised the experiments, and revised the manuscript. All authors read and approved the final manuscript.

Funding

This work is supported by National Natural Science Foundation of China (21808068), National Key R&D Program of China (2018YFA0901000) and Natural Science Foundation of Guangdong province (2018A030313791).

Availability of data and materials

All data generated or analyzed during this study are included in this published article and its additional information files.

Ethics approval and consent to participate

Not applicable.

Consent for publication

All authors agreed to publish this article.

Competing interests

The authors declare that they have no competing interests.

Received: 15 November 2019 Accepted: 17 February 2020

Published online: 27 February 2020

References

1. Beekwilder J, van Rossum HM, Koopman F, Sonntag F, Buchhaupt M, Schrader J, et al. Polycistronic expression of a beta-carotene biosynthetic pathway in *Saccharomyces cerevisiae* coupled to beta-ionone production. *J Biotechnol*. 2014;192:383–92.
2. Gershenzon J, Dudareva N. The function of terpene natural products in the natural world. *Nat Chem Biol*. 2007;3(7):408–14.
3. Leavell MD, McPhee DJ, Paddon CJ. Developing fermentative terpenoid production for commercial usage. *Curr Opin Biotechnol*. 2016;37:114–9.
4. Liu Y, Nielsen J. Recent trends in metabolic engineering of microbial chemical factories. *Curr Opin Biotechnol*. 2019;60:188–97.
5. González-Verdejo CI, Obrero Á, Román B, Gómez P. Expression profile of carotenoid cleavage dioxygenase genes in summer squash (*Cucurbita pepo* L.). *Plant Food Hum Nutr*. 2015;70:200–6.
6. Lalko J, Lapczynski A, McGinty D, Bhatia S, Letizia CS, Api AM. Fragrance material review on trans-beta-ionone. *Food Chem Toxicol*. 2007;45(Suppl 1):248–50.
7. Abdel-Mawgoud AM, Markham KA, Palmer CM, Liu N, Stephanopoulos G, Alper HS. Metabolic engineering in the host *Yarrowia lipolytica*. *Metab Eng*. 2018;50:192–208.
8. Nacke C, Hüttmann S, Etschmann MM, Schrader J. Enzymatic production and in situ separation of natural beta-ionone from beta-carotene. *J Ind Microbiol Biotechnol*. 2012;39(12):1771–8.
9. Berger RG, Zorn H. Flavors and fragrances. Berlin: Springer; 2007.
10. Park SY, Yang D, Ha SH, Lee SY. Metabolic engineering of microorganisms for the production of natural compounds. *Adv Biosyst*. 2018;2:1700190.
11. Vickers CE, Williams TC, Peng B, Cherry J. Recent advances in synthetic biology for engineering isoprenoid production in yeast. *Curr Opin Chem Biol*. 2017;40:47–56.
12. Ma YR, Wang KF, Wang WJ, Ding Y, Shi TQ, Huang H, et al. Advances in the metabolic engineering of *Yarrowia lipolytica* for the production of terpenoids. *Bioresour Technol*. 2019;281:449–56.
13. Krivoruchko A, Nielsen J. Production of natural products through metabolic engineering of *Saccharomyces cerevisiae*. *Curr Opin Biotechnol*. 2015;35:7–15.
14. Cao X, Lv YB, Chen J, Imanaka T, Wei LJ, Hua Q. Metabolic engineering of oleaginous yeast *Yarrowia lipolytica* for limonene overproduction. *Biotechnol Biofuels*. 2016;9:214.
15. Cao X, Wei LJ, Lin JY, Hua Q. Enhancing linalool production by engineering oleaginous yeast *Yarrowia lipolytica*. *Bioresour Technol*. 2017;245:1641–4.
16. Guo X, Sun J, Li D, Lu W. Heterologous biosynthesis of (+)-nootkatone in unconventional yeast *Yarrowia lipolytica*. *Biochem Eng J*. 2018;137:125–31.
17. Nambou K, Jian X, Zhang X, Wei L, Lou J, Madzak C, et al. Flux balance analysis inspired bioprocess upgrading for lycopene production by a metabolically engineered strain of *Yarrowia lipolytica*. *Metabolites*. 2015;5(4):794–813.
18. Larroude M, Celinska E, Back A, Thomas S, Nicaud JM, Ledesma-Amaro R. A synthetic biology approach to transform *Yarrowia lipolytica* into a competitive biotechnological producer of β -carotene. *Biotechnol Bioeng*. 2018;115(2):464–72.
19. Kildegaard KR, Adiego-Pérez B, Doménech Belda D, Khangura JK, Holkenbrink C, Borodina I. Engineering of *Yarrowia lipolytica* for production of astaxanthin. *Synth Syst Biotechnol*. 2017;2(4):287–94.
20. Martin VJ, Pitera DJ, Withers ST, Newman JD, Keasling JD. Engineering a mevalonate pathway in *Escherichia coli* for production of terpenoids. *Nat Biotechnol*. 2003;21(7):796–802.
21. Pfleger BF, Pitera DJ, Smolke CD, Keasling JD. Combinatorial engineering of intergenic regions in operons tunes expression of multiple genes. *Nat Biotechnol*. 2006;24(8):1027–32.

22. Ajikumar PK, Xiao WH, Tyo KE, Wang Y, Simeon F, Leonard E, et al. Isoprenoid pathway optimization for Taxol precursor overproduction in *Escherichia coli*. *Science*. 2010;330:70–4.
23. Zhang C, Chen X, Lindley ND, Too HP. A “plug-n-play” modular metabolic system for the production of apocarotenoids. *Biotechnol Bioeng*. 2018;115(1):174–83.
24. Zhang C, Seow VY, Chen X, Too HP. Multidimensional heuristic process for high-yield production of astaxanthin and fragrance molecules in *Escherichia coli*. *Nat Commun*. 2018;9(1):1858.
25. Zhou YJ, Gao W, Rong Q, Jin G, Chu H, Liu W, et al. Modular pathway engineering of diterpenoid synthases and the mevalonic acid pathway for multiradiene production. *J Am Chem Soc*. 2012;134(6):3234–41.
26. Qin J, Zhou YJ, Krivoruchko A, Huang M, Liu L, Khoomrung S, et al. Modular pathway rewiring of *Saccharomyces cerevisiae* enables high-level production of L-ornithine. *Nat Commun*. 2015;6:8224.
27. Gibson DG, Young L, Chuang RY, Venter JC, Hutchison CA, Smith HO. Enzymatic assembly of DNA molecules up to several hundred kilobases. *Nat Methods*. 2009;6(5):343–52.
28. Gao S, Tong Y, Wen Z, Zhu L, Ge M, Chen D, et al. Multiplex gene editing of the *Yarrowia lipolytica* genome using the CRISPR–Cas9 system. *J Ind Microbiol Biotechnol*. 2016;43(8):1085–93.
29. Zhang JL, Peng YZ, Liu D, Liu H, Cao YX, Li BZ, et al. Gene repression via multiplex gRNA strategy in *Y. lipolytica*. *Microb Cell Fact*. 2018;17(1):62.
30. Czajka JJ, Nathenson JA, Benites TV, Baidoo EEK, Cheng Q, Wang Y, et al. Engineering the oleaginous yeast *Yarrowia lipolytica* to produce the aroma compound beta-ionone. *Microb Cell Fact*. 2018;17(1):136.
31. Yuan JC, Ching CB. Mitochondrial acetyl-CoA utilization pathway for terpenoid productions. *Metab Eng*. 2016;38:303–9.
32. Huang YY, Jian XX, Lv YB, Nian KQ, Gao Q, Hua Q, et al. Enhanced squalene biosynthesis in *Yarrowia lipolytica* based on metabolically engineered acetyl-CoA metabolism. *J Biotechnol*. 2018;281:106–14.
33. Ignea C, Trikka FA, Nikolaidis AK, Georgantea P, Ioannou E, Kampranis SC, et al. Efficient diterpene production in yeast by engineering Erg20p into a geranylgeranyl diphosphate synthase. *Metab Eng*. 2015;27:65–75.
34. Bergman A, Siewers V, Nielsen J, Chen Y. Functional expression and evaluation of heterologous phosphoketolases in *Saccharomyces cerevisiae*. *AMB Express*. 2016;6:115.
35. Schwartz CM, Hussain MS, Blenner M, Wheeldon I. Synthetic RNA polymerase III promoters facilitate high-efficiency CRISPR–Cas9-mediated genome editing in *Yarrowia lipolytica*. *ACS Synth Biol*. 2016;5(4):356–9.
36. Gao S, Tong Y, Zhu L, Ge M, Zhang Y, Chen D, et al. Iterative integration of multiple-copy pathway genes in *Yarrowia lipolytica* for heterologous beta-carotene production. *Metab Eng*. 2017;41:192–201.
37. Matthäus F, Ketelhot M, Gatter M, Barth G. Production of lycopene in the non-carotenoid-producing yeast *Yarrowia lipolytica*. *Appl Environ Microbiol*. 2014;80(5):1660–9.
38. Qiao K, Wasylenko TM, Zhou K, Xu P, Stephanopoulos G. Lipid production in *Yarrowia lipolytica* is maximized by engineering cytosolic redox metabolism. *Nat Biotechnol*. 2017;35(2):173–7.
39. Madzak C, Tréton B, Blanchin-Roland S. Strong hybrid promoters and integrative expression/secretion vectors for quasi-constitutive expression of heterologous proteins in the yeast *Yarrowia Lipolytica*. *J Mol Microbiol Biotechnol*. 2000;2(2):207–16.
40. Ledesma-Amaro R, Dulermo T, Nicaud JM. Engineering *Yarrowia lipolytica* to produce biodiesel from raw starch. *Biotechnol Biofuels*. 2015;8:148.
41. Marella ER, Dahlin J, Dam MI, Ter Horst J, Christensen HB, Borodina I, et al. A single-host fermentation process for the production of flavor lactones from non-hydroxylated fatty acids. *Metab Eng*. 2019 (in press).
42. Larroude M, Rossignol T, Nicaud JM, Ledesma-Amaro R. Synthetic biology tools for engineering *Yarrowia lipolytica*. *Biotechnol Adv*. 2018;36(8):2150–64.
43. Markham KA, Alper HS. Synthetic biology expands the industrial potential of *Yarrowia lipolytica*. *Trends Biotechnol*. 2018;36(10):1085–95.
44. Werner N, Ramirez-Sarmiento CA, Agosin E. Protein engineering of carotenoid cleavage dioxygenases to optimize β -ionone biosynthesis in yeast cell factories. *Food Chem*. 2019;299:125089.
45. Markham KA, Palmer CM, Chwatko M, Wagner JM, Murray C, Vazquez S, et al. Rewiring *Yarrowia lipolytica* toward triacetic acid lactone for materials generation. *Proc Natl Acad Sci USA*. 2018;115(9):2096–101.
46. Chen G, Fan KW, Lu FP, Li Q, Aki T, Chen F, et al. Optimization of nitrogen source for enhanced production of squalene from thraustochytrid *Aurantiochytrium* sp. *New Biotechnol*. 2010;27(4):382–9.
47. Khadka N, Farquhar ER, Hill HE, Shi W, von Lintig J, Kiser PD. Evidence for distinct rate-limiting steps in the cleavage of alkenes by carotenoid cleavage dioxygenases. *J Biol Chem*. 2019;294(27):10596–606.
48. Chang MC, Eachus RA, Trieu W, Ro DK, Keasling JD. Engineering *Escherichia coli* for production of functionalized terpenoids using plant P450s. *Nat Chem Biol*. 2007;3(5):274–7.
49. Paddon CJ, Westfall PJ, Pitera DJ, Benjamin K, Fisher K, McPhee D, et al. High-level semi-synthetic production of the potent antimalarial artemisinin. *Nature*. 2013;496(7446):528–32.
50. Luo X, Reiter MA, d’Espaux L, Wong J, Denby CM, Lechner A, et al. Complete biosynthesis of cannabinoids and their unnatural analogues in yeast. *Nature*. 2019;567(7746):123–6.
51. Simkin AJ, Underwood BA, Aldridge M, Loucas HM, Shibuya K, Schmelz E, et al. Circadian regulation of the PhCCD1 carotenoid cleavage dioxygenase controls emission of β -ionone, a fragrance volatile of petunia flowers. *Plant Physiol*. 2004;136(3):3504–14.
52. Schwartz C, Shabbir-Hussain M, Frogue K, Blenner M, Wheeldon I. Standardized markerless gene integration for pathway engineering in *Yarrowia lipolytica*. *ACS Synth Biol*. 2017;6(3):402–9.
53. Nicaud JM, Madzak C, van den Broek P, Gysler C, Duboc P, Niederberger P, et al. Protein expression and secretion in the yeast *Yarrowia lipolytica*. *FEMS Yeast Res*. 2002;2(3):371–9.
54. Xue Z, Sharpe PL, Hong SP, Yadav NS, Xie D, Short DR, et al. Production of omega-3 eicosapentaenoic acid by metabolic engineering of *Yarrowia lipolytica*. *Nat Biotechnol*. 2013;31(8):734–40.

Publisher's Note

Springer Nature remains neutral with regard to jurisdictional claims in published maps and institutional affiliations.

Ready to submit your research? Choose BMC and benefit from:

- fast, convenient online submission
- thorough peer review by experienced researchers in your field
- rapid publication on acceptance
- support for research data, including large and complex data types
- gold Open Access which fosters wider collaboration and increased citations
- maximum visibility for your research: over 100M website views per year

At BMC, research is always in progress.

Learn more biomedcentral.com/submissions

